Characterization of Uncertainty Sources of Special Core Analysis

André Luiz Martins Compan[1], *Caroline Henrique* Dias[2], *Rodrigo* Surmas[1] and *Flavia Barros* de Andrade[1]

[1]PETROBRAS, CENPES, CEP 21941-915 - Rio de Janeiro, RJ - Brasil
[2]UFRJ, LRAP, CT2, CEP 21941-914 - Rio de Janeiro - RJ – Brasil

Abstract. Special Core Analyses (SCAL) involve intricate measurements with various sources of uncertainty, both evident and subtle. While pressure transducers and flowmeters contributions are clear, factors such as dead volumes, delays in measuring produced volumes and pressures, and compressibility of flow lines present hidden challenges. Additionally, unique issues like fractional flow in outlet pipelines, fluid trapping, and line leakage further complicate the analyses. These uncertainties may correlate, and isolated propagation could overestimate confidence intervals. To address this, covariance between variables must be considered, using either prior knowledge or scenario simulations through methods like Monte Carlo. Analytical approaches offer quick results and insight into interdependencies, aiding the identification and mitigation of critical uncertainty sources. However, over- or underestimating confidence intervals remain a risk if interdependence is poorly understood. For properties derived through optimization, such as transient regime relative permeability curves, numerical methods are more suitable as they surpass analytical approaches in reliability and utility. This study delivers a comprehensive analysis of uncertainty sources and their interdependencies, proposing an analytical framework for uncertainty propagation. Additionally, it emphasizes numerical methodologies for determining robust confidence intervals in scenarios where analytical methods are limited. The integration of both techniques enhances SCAL reliability and accuracy.

1 Introduction

Every measurement inherently has associated uncertainties; therefore, no measurement should be reported without its accompanying uncertainty. Furthermore, the corrected evaluation of the NPV (Net Present Volume) and the NP (Net Production) and their uncertainties is very important to avoid decision errors and disappointments [1]. However, in certain cases, evaluating uncertainty is highly complex. Special Core Analysis (SCAL) uncertainties are undoubtedly complex, particularly relative permeability is really challenging [2]; however, from a pragmatic perspective, it is possible to estimate an approximate level of uncertainty in the analyses. The objective of this text is to establish a preliminary approach to determining the uncertainty in SCAL analyses, evaluating many sources of uncertainty and its impact on SCAL measurements.

As Pore Volume and Absolute Permeability are used in the special core analysis they will be addressed as well.

In addition to evaluating experimental uncertainties, it is important to assess the uncertainty resulting from the interpretation process of these data for generating the curve, especially in transient regime cases where determining the curve does not result directly from raw data applied to a mathematical equation. The uncertainty of processing test data in the transient regime is addressed only preliminarily in this text, as it requires more extensive ongoing research and will be explored in future projects.

Evaluating uncertainty through systematic repetition of tests (Type A uncertainty evaluation [3]) is simpler to obtain and robust in one aspect: it does not rely on modeling the variables affecting the process, which might be incomplete or flawed. However, it is less robust regarding variability across cases: after a set of tests with a specific sample under particular conditions, one arrives at an uncertainty associated with that sample and those conditions. Such uncertainty would not be valid for distinct conditions (different fluids, different temperatures) or a different sample (much smaller, larger, more/less permeable), or even the same sample if it had been altered between experiments.

In cases of analyses involving large volumes without significant variation in conditions/samples, this type of statistical uncertainty evaluation is advisable. However, this is not the case here, where repeating the same test in sufficient quantity for statistically representative uncertainty/repeatability is infeasible, and the samples might be affected by the test, conditioning, or handling.

On the other hand, the evaluation presented here (Type B uncertainty evaluation [3]), if the model is accurate, would predict the confidence interval, as this (except for gross or systematic errors) results from measured and included associated uncertainties. In other words, the repetition of an analysis, with a certain level of confidence, should fall within the estimated confidence interval.

Data used in simulation cells involve at least three levels of uncertainties cumulatively. The first level refers to laboratory measurement (or Digital Rock Physics characterization) uncertainty for the property of a specific rock sample. The second level involves the property variability within a “similar” samples group (rocktyping). The third level concerns uncertainty in upscaling from sample scale (after rocktyping) to simulation cell scale. This article aims to provide a broad range of uncertainty sources and to describe methodologies for determining uncertainties in laboratory measurements (the first level mentioned).

* Corresponding author: andrecompan@petrobras.com.br

2 General Sources of Uncertainty

2.1 Transducers Precision

Measuring instruments are typically marketed with predefined uncertainty specifications. However, for a more robust precision estimation, the calibration process should include the development of a calibration curve that correlates the instrument's direct response (e.g., voltage or current) to the desired measurement parameter (e.g., pressure, differential pressure, temperature, mass, flow rate). This curve should encompass multiple calibration points distributed across the instrument's measurement range. Such an approach allows for the determination of a regression model and the establishment of confidence intervals for the measurements, as outlined by De Groot and Schervish [5].

2.2 Sample Geometry

The interpretation of most petrophysical tests assumes that the sample possesses a perfectly cylindrical geometry. However, imperfections in the sample's geometry introduce uncertainties into the measured properties. This study does not address how various geometric imperfections, such as lack of perpendicularity, lack of parallelism of flow faces, ovalization, conicity, and surface irregularities, impact the estimated properties, as cylindrical samples are generally deemed sufficiently accurate, nevertheless, it should be studied with more detail in the future. Instead, the focus here is on the uncertainties associated with the fundamental geometric properties of the cylinder itself: diameter and length.

Measuring these geometric properties is typically a straightforward and fast process. This enables the inference of uncertainties based on repeated measurements (using calibrated equipment with high accuracy). Nevertheless, it is recommended to perform more than 30 repetitions to ensure adequate statistical representation (for a normally distributed property, 30 observation result in a 13% difference between the standard deviation of the experimental standard deviation of the mean relative to the standard deviation of the mean [3]). However, such a procedure may be impractical in routine laboratory workflows. An alternative approach is to work with the propagation of individual measurement uncertainties (arising from the calibration of measuring instruments against calibration standards, for instance) to the target property value.

Traditional measurement methods, such as those using calipers, introduce an additional source of error that is not captured by the uncertainty specifications of the instruments themselves. This operational error includes factors such as variations in the pressure applied to the instrument and improper alignment during measurement. While these types of errors can be captured when uncertainty is estimated through statistically representative repetition (Type A), they are not accounted for in the propagation of uncertainties to the target property value. Proper training of laboratory personnel and the use of measuring instruments that are less susceptible by operational errors are critical for mitigating these issues.

Beyond operational errors, some geometry flaws like the lack of perpendicularity or parallelism can also introduce uncertainties due to the creation of void volumes or unaccounted dead volumes, as well as operational issues such as the loss of confinement sleeves.

2.3 Confining Pressure

It is widely recognized that confining pressure has a significant impact on various special core analysis properties. However, this is primarily a matter of representativeness rather than measurement uncertainty, unless the absence of enough confining pressure leads to a flow bypass through the space between the sleeve and the sample.

One aspect worth discussing is how the uncertainty in confining pressure measurements might affect the representativeness of the results. Specifically, as the measured property usually is intended to be representative of a specific confining pressure condition, but the actual applied condition carries uncertainty, the sensitivity of the property to confining pressure propagates this uncertainty into the measured property.

Another important consideration is the very definition of representative confining pressure. Determining the most representative hydrostatic confining pressures to reflect the in-situ stress state of reservoir rocks involves various uncertainties and simplifications. However, this aspect lies beyond the scope of the present study

2.4. Pore Geometry Changes

Standard petrophysical characterization should be conducted on rocks whose porous geometry remains unchanged throughout the testing process (if variations in porous geometry are critical to the process, they should be addressed separately). However, certain interactions between the rock and the fluids used, such as dissolution and precipitation, clay swelling, movement of fines and grains, and rock compaction (under the same pressure conditions), can significantly impact both basic and special petrophysical properties, changing pore volumes, permeabilities, and pore distribution.

While these phenomena may be considered more as errors or issues in the testing process rather than uncertainties, awareness of these sources of variation in measured properties is essential.

2.5. Density and Viscosity

Viscosity and density can be obtained through two main approaches:

1. estimation using established correlations
2. direct measurement.
   - 2.1. measured independently of the analysis where the information will be used
   - 2.2. measured under the same conditions and at the same time the analysis is being conducted.

In situations where viscosity and density are measured or applied directly, the calibration of the instrument becomes the primary source of input uncertainty in the propagation process, as discussed in Section 2.1.

If viscosity and density are measured beforehand or estimated using correlations, they are typically defined as functions of pressure and temperature. In this case, uncertainties in the measurement of pressure and temperature must be propagated to the final result, along with the inherent uncertainty of the density or viscosity correlation with respect to temperature and pressure.

2.6. Pressure Drop

The measurement of absolute and effective permeability relies on determining the pressure drop between the inlet and outlet faces of the sample (in some equipment, it is also possible to assess pressure along the sample; the uncertainty associated with this type of measurement is beyond the scope of this text). Certain equipment, particularly those used for gas flow measurements to determine absolute permeability, measures pressure at a certain distance from the sample face. In these cases, there is a pressure drop between the sample face and the pressure measurement point that needs to be modeled, introducing uncertainties into the measurement.

In single-phase flows, this modeling can be performed by measuring the pressure drop in the inlet and outlet sections under varying flow rate and pressure conditions, then applying the modeled pressure drop under the conditions of the test. In addition to the uncertainty associated with the regression used in the modeling, the propagation of uncertainties in pressure and temperature measurements during the test must also be considered in the estimation of the pressure drop.

A simplified modeling approach involves measuring the total pressure drop (inlet and outlet) using the differential pressure sensor of the equipment in an analysis without the rock sample. The total pressure drop must then be distributed between the inlet and outlet sections based on secondary modeling, which introduces additional uncertainties.

In non-single-phase scenarios, the situation becomes more challenging, as saturation, phase distribution, flow pattern and fluid positioning within the tubing impacts the pressure drop, making the modeling significantly less precise.

2.7. Inlet and Outlet Headers

Holder headers serve as flow distributors at the inlet face and flow collectors at the outlet face. One of their roles is to ensure the most homogeneous distribution of flow across the sample faces, avoiding significant pressure gradients or regions with inadequate fluid supply. Since this phenomenon is still being evaluated, no method is proposed in this paper to estimate the uncertainty resulting from the lack of pressure homogeneity at the inlet and outlet due to the headers. Some authors propose additional features to ensure the homogeneity of injection/collect flow like discarding sections of the sample or using metal mesh after the diffusor [4]

Another critical characteristic of headers is avoiding fluid entrapment during flow, which would primarily impact saturation measurements. In saturation evaluations, it can be considered that part of the volume in the grooves of the headers contributes to saturation uncertainty. The percentage to be accounted for will depend on the flow behavior within each header design, and the impact on the final result will depend on the ratio between the porous volume of the sample and the volume of the header grooves.

2.8. Dead Volumes

Dead volumes refer to fluid regions that delay or impact pressure and production measurements in non-single-phase flows. In this study, they are categorized into three groups: delay volumes, excess volumes, and contact volumes, as described below and shown in fig.1.

1. **Delay volumes** represent regions where the fluid present does not affect the quantity of the monitored production fluid (typically the fluid present is the same fluid being injected into the sample) but introduces a delay between the moment the produced fluid exits the sample and the moment it is accounted for by a measurement method.

2. **Excess volumes** consist of additional fluid that is included in the monitored production and needs to be subtracted from the production data. It is possible for fluid volumes in the system to simultaneously act as both excess and delay volumes.

3. **Contact volumes** consist of fluid regions that are in contact with the main flow but should not be produced. However, due to differences in density, instability at fluid interfaces, or pressures induced by the flow, these fluids may be produced, affecting both the timing of monitored production and the monitored volume. Common locations for these fluids included within multi-way valves, headers with multiple inlets, and pressure taps.

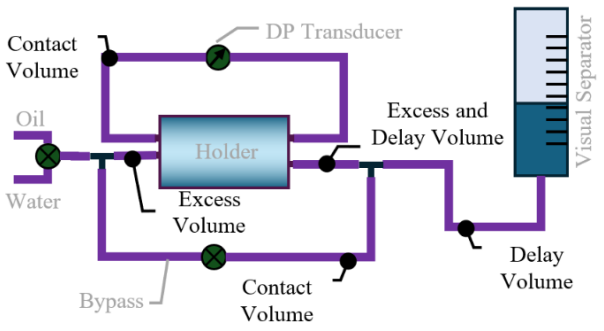

Fig. 1. Dead Volumes Scheme for an Unsteady State water-oil relative permeability test

Delay and excess dead volumes must be measured and used to correct production times and volumes. They can be measured by flowing sequence of immiscible fluids through the tubing filled, measuring the displaced volume, or by using gas expansion (the same way the porosity is usually measured). Larger dead volumes result in greater uncertainties that propagate to the final results.

Contact dead volumes should ideally not be produced and therefore should not be accounted for. However, depending on the design of the equipment and the flow conditions, they may be partially or fully produced, resulting in an additional source of uncertainty/error to the results.

2.9. Tilted Bedding

The inclination of layers relative to the sample axis introduces an artifact, as the imposed flow through inclined layers, driven by the sample confinement, creates a scenario that deviates from the reservoir's reality, affecting both the pressure differential and the actual sweep, as shown in fig.2.

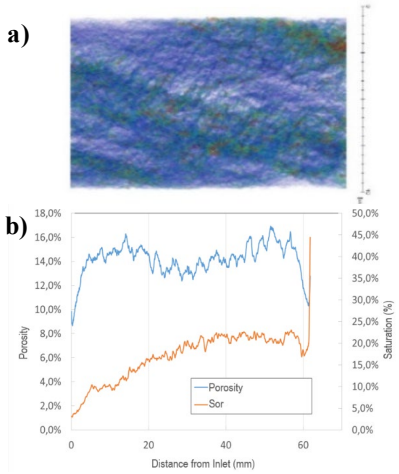

Fig. 2. Tomographic imaging and determination of porosity and residual oil saturation through tomographic imaging in non-parallel bedding sample showing an increase in oil saturation due to sweep efficiency artifact.

The saturation map (fig.2a) shows oil residue (green color) increased in a probable (the imaging was done after the injection, in a static condition) stagnated corner of the sample. The saturation profile (fig. 2b) shows a different trend between porosity and oil saturation, that can be partially result of boundary end effects, but as shown in the saturation map, is, at least partially, influenced by the layering.

2.10. Sample Heterogeneity

Most SCAL tests treat samples as black boxes, without accounting for internal variability in properties and physical states, such as saturation, pressure, salinity concentration, among others. The interpretation of raw test data is typically performed under the assumption of property homogeneity, using modeling approaches that rely on this assumption.

Sample heterogeneity can lead to modeling failures, errors, and uncertainties in the characterized properties. It is not possible to establish confidence intervals to adequately address deviations from the optimal scenario. Therefore, it is recommended to exercise caution in sample selection, incorporating microtomographic image analysis during the screening phase. Additionally, when heterogeneity cannot be avoided within the facies being characterized at the laboratory sample scale, it is advisable to include information on the distribution of properties and states (like saturation maps during the test) during data acquisition and the experimental modeling of the heterogeneous sample.

3 Routine Core Analysis

In addition to the sources of uncertainty mentioned earlier, some are specific to each technique. This section will describe specific sources of uncertainty associated with Routine Core Analysis.

3.1. Absolute Permeability

3.1.1 Klinkenberg Estimation

The property required for reservoir rock characterization is absolute permeability (k_{ABS}), which is an intrinsic property of the rock and independent of the type and pressure of fluids. However, the gas permeability depends on the pressure used to measure the permeability, resulting in a "apparent permeability" (k_{AP}). Klinkenberg [6] modelled this behavior and his model can be used to "convert" the apparent permeability in the absolute permeability.

Absolute permeability can be measured using several main approaches:

1. Performing multiple steady-state measurements of apparent permeabilities at different pressures and using linear regression to obtain absolute permeability (and the Klinkenberg parameter);
2. Repeating the procedure described in item 1 across multiple samples of a specific rock type to determine a representative Klinkenberg parameter for that rock type as a function of absolute permeability, and applying this parameter to similar rocks to avoid repeated tests when a large number of analyses are required;
3. Utilizing literature correlations (fig.3) to estimate the Klinkenberg parameter as a function of absolute permeability and applying this parameter to convert apparent permeability into absolute permeability;
4. Measuring gas permeability under transient flow conditions and modeling the pressure decay process, incorporating the Klinkenberg effect to determine absolute permeability and the Klinkenberg parameter that fits the pressure history;
5. Directly measuring permeability using liquids.

Each method for measuring and calculating absolute permeability has its own sources of uncertainty and specificities. The linear regression method, based on multiple apparent permeability measurements from the same sample, involves uncertainties related to the measurement of apparent permeability itself, the measurement and calculation of mean gas pressure, the Klinkenberg model itself, and the linear regression process.

When calculations rely directly on the Klinkenberg parameter modeled for similar samples, like in methods 2 and 3, above, additional uncertainty arises from the

"rocktyping" process. Using literature regressions introduces greater dispersion as the definition of "similarity" for rock typing becomes less restrictive. Therefore, estimates using literature data are generally more uncertain than correlations derived from samples within the same reservoir or area.

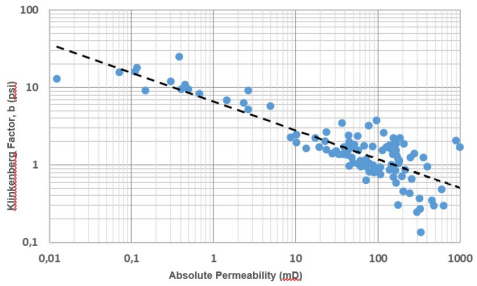

Fig. 3. Klinkenberg Parameter and absolute permeability correlation from Jones S.C. [7].

3.1.2 Forcheimmer Effect

Darcy's law is valid for laminar flows, but at higher flow velocities, second-order effects can influence the relationship between flow potential and flow rate. At low flow rates, these second-order effects are generally negligible. However, as flow rates increase, deviations from Darcy's linearity can impact uncertainty if modeling continues to assume the linear relationship predicted by Darcy's law. The impact of deviations from Darcy's predicted linearity will not be evaluated in this study but should be addressed in future work.

3.2. Porosity and Grain Density

3.2.1 Void Volumes

Measurements of porosity and grain density typically rely on the determination of void volumes within a system to calculate pore volumes and solid volumes. The most commonly used method for void volume measurement involves applying the ideal gas law (PV = nRT) during gas expansion processes. In each expansion process, measurements are conducted at three distinct locations: 1) In the reference chamber and lines, before the expansion; 2) In the lines and sample location, before the expansion; 3) In the total system combining both (1+2), after the expansion.

The void volume (V_v) is then calculated by:

$$V_v = V_1 \frac{\frac{P_1}{T_1} - \frac{P_3}{T_3}}{\frac{P_3}{T_3} - \frac{P_2}{T_2}} \quad (1)$$

The numerical indexes represent the three possible locations/moments mentioned above.

To calculate pore volume or solid volume, it is necessary to measure or define pressures, volumes, and temperatures six times (three locations/moments - 1, 2 and 3 at the equation 1 - with and without the sample in the system).

The volume of reference chambers and lines (V_1) is typically calibrated beforehand, and its uncertainties must be quantified during the calibration process. The lines and void spaces connected to the sample location can either be calibrated beforehand or evaluated using two consecutive void volume measurements, with and without the sample in the system. The pressure at the sample location (P_2) is often not measured but assumed to be atmospheric (Patm). If proper precautions are not taken to avoid residual pressures at this position, measurement errors may be introduced. Regardless, there is uncertainty in P_2 when it is measured and an exacerbated uncertainty when it is assumed as P_{atm}.

An additional source of uncertainty beyond those associated with the measuring instruments is the representativeness of the temperature measurements. Ideally, the temperatures should reflect the condition of the gas; however, temperature sensors are often not in direct contact with the gas but rather positioned in the laboratory environment, the equipment surroundings, or the external wall of the gas tube or cylinder. Even if the temperature were measured directly in the gas, spatial temperature variations could occur, for example, between the sections inside and outside the equipment.

3.2.2 Additional Masses

Another source of uncertainty that must be considered in porosity and grain density measurements arises from the inclusion of materials added to the sample, such as encapsulating sleeves and materials used to remove surface irregularities. Each added material must be accounted for in the calculation, introducing uncertainties related to their masses and volumes.

3.2.3 Porous Volume by Weight

It's possible to calculate the pore volume by weight (as shown in Equation 2). It is representative of a non-confining state and can be more suitable for non-confining tests like centrifuge capillary pressure, for instance.

$$V_{pp} = \frac{m_{sat} - m_{dry}}{\rho_{sat}} \quad (2)$$

Where m_{sat} e m_{dry} are respectively the mass of the liquid-saturated sample (which will be displaced during centrifugation) and ρ_{sat} is the density of the saturating fluid.

Besides the uncertainty propagated from the sources of data used in the Equation 2, this kind of pore volume estimation has additional sources of uncertainty due to the trapped gas and solution gas (not presented when ρ_{sat} was measured).

4 Special Core Analysis

4.1. General Sources of SCAL Uncertainties

4.1.1 Capillary End Effects

Special Core Analysis tests typically involve two fluids, often immiscible, which result in capillary pressures and

wettability effects within the sample and at the interface between the sample and the external medium (diffusors fluid conduits).

Internal capillary effects, if the physical conditions are similar to those observed in the reservoir, are representative of the reservoir behavior. However, capillary effects at the interface between the sample and the external medium would only be representative of specific regions of the reservoir, such as the interface with the wellbore wall, open fractures, or cavities. Thus, sample edges capillary effects are considered laboratory artifacts and must be corrected during property characterization. This correction introduces uncertainties related to the modelling of the phenomenon, the homogeneity of the sample, and the measurements required for the model calculations, such as the representative capillary pressure of the porous medium.

Uncertainty in capillary pressure can be incorporated by accounting for it during the history-matching process of laboratory tests, like in multi-rate unsteady state relative permeabilities tests.

4.1.2 Production Completeness

Fluid displacement in tests such as relative permeability and capillary pressure can be very slow, and complete production (no displaced fluid production, evaluated by the production tendency over time) may not be achieved within timeframes that meet the demand for timely information. Consequently, in some cases, experiments are concluded under conditions where production, despite having ceased for some time, clearly remains at a non-negligible distance from its asymptote, as observed in the production curve behavior.

This production uncertainty can be significant since there is no clear threshold to determine the achievement of complete production. In infinite time or infinite pressure scenarios, extrapolating the production trend could lead to saturation values approaching zero. However, practical limits exist, such as maximum pressure and time in capillary pressure tests, fractional flows, injected porous volumes, and time in relative permeability tests, where additional production would no longer be relevant to the reservoir.

Analytical approaches or history marching may attempt to propose extrapolations of the production curve, taking care not to select extrapolations that lead to unreasonable scenarios. To incorporate uncertainties, multiple extrapolations can be evaluated, ensuring they fit the data while yielding distinct production outcomes.

4.2. Relative Permeability

4.2.1 Fluids, Tubing and Pore Compressibility

In relative permeability tests, the pressures applied to fluids, tubing, and the porous medium can be significant and may result in volume changes due to the compressibility of these components.

Volume variations can lead to saturation errors if not accounted for, or to propagated uncertainties if considered, arising from pressure measurements and compressibility characterization.

For example, dead volumes are typically measured under a specific fluid pressure condition. If the tests are conducted under different pressure conditions, the dead volumes will be affected, with greater impact as the dead volumes and the compressibility of the tubing increase.

Production measurements performed under conditions different from those of the fluids in the sample also need to be corrected using the appropriate Formation Volume Factor (FVF). While this correction is generally performed, it introduces uncertainties propagated from pressure measurements and the uncertainty associated with the fluid's Formation Volume Factor.

Using a sample at a pressure different from that used to calculate its reference pore volume, or changes in the pore volume during the relative permeability test, also requires production corrections. As with any correction, this introduces uncertainties propagated from the primary sources.

4.2.2 Relative Permeability Reference

The permeability presented in the curves is the relative permeability relative to a certain reference permeability. Therefore, relative permeability includes an additional source of uncertainty: the uncertainty of reference permeability. If the reference is the effective permeability to oil itself, the relative permeability at the initial point is, by definition, Kro = 1, meaning there is no additional propagation of uncertainty stemming from this definition. Nevertheless, even if the laboratory curve has been referenced by Kro at the initial point, to apply the information at the reservoir cell the reference with the Absolute Permeability needs to be set somewhere along the upscaling process.

4.2.3 Gravitational Divergence

When relative permeability tests are conducted in a horizontal orientation, it is generally assumed that, due to the sample's small size, there is no significant tendency for fluid separation based on density. This assumption is typically applied to fluids with similar densities, such as water and oil. Tests involving gas at low pressures are commonly conducted with the sample positioned vertically, as the non-divergence assumption does not appear valid. However, even in water and oil scenarios, it is reasonable to assume that some level of divergence may occur. This source of uncertainty will not be explicitly addressed in this study, but it should be considered in future evaluations.

Implicitly, density differences can be factored into the uncertainty by incorporating the sample's inclination angle relative to the horizontal as a source of uncertainty. This approach does not directly evaluate gravitational divergence, which can occur even with a perfectly horizontal sample, but by accounting for uncertainty in the sample's tilt, an estimate of divergence uncertainty may be indirectly introduced.

4.3. Centrifuge Capillary Pressure

4.3.1 Capillary Pressure

The capillary pressure in the analysis using the centrifuge is based on a direct calculation described in equations 3 and 4 for a specific point of the sample.

The capillary pressure is at its maximum at the face where the displacing fluid enters the sample and is given, in the case of a less dense displacing fluid, by:

$$P_c = \frac{1}{2}\omega^2 \Delta\rho \left({R_{out}}^2 - {R_{in}}^2\right) \quad (3)$$

And, in the case of a denser displacing fluid,

$$P_c = \frac{1}{2}\omega^2 \Delta\rho \left({R_{in}}^2 - {R_{out}}^2\right) \quad (4)$$

This calculation and the associated measurements have various sources of uncertainty. The density of the fluids is one of them, as mentioned in section 2.5. Additionally, there is uncertainty related to the rotation used in centrifugation, which is associated with measurement uncertainty and the imposition of rotation, i.e., errors in the control of the centrifuge's rotational speed, as well as uncertainty related to the outer and inner radii resulting from the flattening or deformation of the cups, non-standard assembly, sample irregularities, and measurements taken at an angle.

4.3.2 Saturation

Saturation is another critical point in estimating the capillary pressure curve and is susceptible to a large number of sources of uncertainty.

The main sources of uncertainty in measuring saturation are related to the density of the displaced fluid, the porous volume by weight used as a reference for obtaining saturation, parallax error, which is a reading uncertainty also associated with the length-volume conversion in manually performed readings on scales. When volume readings are conducted using cameras, the reading uncertainty will be related to the camera resolution (pixel size), the pixel-volume conversion, and the accuracy of the reading at the interface between the fluids.

4.3.3 Reading Uncertainty

For the determination of saturation associated with capillary pressure through centrifugation, calibrated cups are utilized. Half of the smallest scale division is regarded as its maximum precision, if measuring the production visually, or the volume measured by the camera pixel length, if measuring the production using a camera. In this type of measurement, there is a conversion between the measured length and the associated volume, thus the reading error in volume varies according to the scale's precision; which is constrained by human visual capability when readings are taken with the naked eye; and is also dependent on the length-volume conversion that varies based on the containers employed.

4.3.4 Parallax Error

In any visual measurement of lengths, which is the case for indirect volume readings based on the meniscus position in the production collector, there exists the issue of parallax, which is exacerbated in the centrifuge by the difficulty of positioning for accurate reading.

The parallax in volume (ℓ_{pV}) is calculated by:

$$\ell_{pV} = \frac{\pi\ \ell_l}{4}\ \frac{{d_{ic}}^2\ (d_{ec} - d_{ic})}{2d_l + \ (d_{ec} - d_{ic})} \quad (5)$$

Where d_{ic} is the internal diameter of the cup, d_{ec} the external diameter of the cup, ℓ_l the deviation from the correct reading position, d_l the distance from the cup to the measurement reader.

4.3.5 Uncertainty of length-volume conversion

The collection cups for produced fluid and reading have a linear scale that indicates how far the meniscus between two fluids is from a reference point. This distance is associated with a certain volume of fluid displaced as a function of the cross-sectional area open for fluid collection.

The cups used in centrifugation have variation in the value of the cross-sectional area in relation to the reference value (used for length-volume conversions) and also in relation to their position along the axis of the cup.

Another aspect that can affect this uncertainty is the pressure on the cup (due to the rotation of the centrifuge) and the temperature of the centrifugation environment (which can affect the area due to the expansion of materials, but also due to changes in pressure resistance).

4.3.7 Modeling uncertainty

The centrifugation technique does not directly measure capillary pressure curves but uses mathematical models to deduce them from experimental measurements.

To obtain the fluid saturation at the face of the sample where the capillary pressure (Pc) is maximum, the relationship between average saturation and point saturation is used, given by:

$$\bar{S_f} = \frac{1}{R_{out} - R_{in}} \int_{R_{in}}^{R_{out}} S(R)dR \quad (6)$$

It is not possible to invert Equation 6 to obtain point saturation directly, as it is a first kind Volterra integral [8]. Many of the methods proposed in the literature use approximations of the saturation equation, with varying degrees of accuracy, which can introduce additional uncertainties to the saturation estimates, as shown by Forbes [9].

The main sources of uncertainty introduced by solving Equation 6 are the assumption of null capillary pressure at the fluid outlet face; the assumption of sample homogeneity; the use of parameterized curves for model

fitting; the assumption of constant saturation in planes parallel to the faces of the sample or correction of radial effects; the assumption of constant saturation in the vertical direction of the sample or correction of gravitational effects; and uncertainties in the geometry of the sample and the rotation radii.

5 Uncertainty Propagation (Analytical Approach)

The propagation of uncertainties is calculated based on the sensitivity of the quantified characteristic in relation to the measured variables and their uncertainties:

$$\sigma_{f(x)}{}^2 = \sum_i \left(\frac{\partial f(x)}{\partial x_i} \sigma_{x_i} \right)^2 \tag{7}$$

In the case of fitting correlations, according to De Groot & Schervish [5], in addition to the propagation of uncertainties in the data (σ_{x_i}), it is also necessary to incorporate the uncertainties of the fitting parameters (σ_{β_j}) and their covariances ($cov(\beta_j \beta_k)$):

$$\sigma_{f(x,\beta)}{}^2 = \sum_i \left(\frac{\partial f}{\partial x_i} \sigma_{x_i} \right)^2 + \sum_j \left(\frac{\partial f}{\partial \beta_j} \sigma_{\beta_j} \right)^2 + 2 \sum_{j,k} \frac{\partial f}{\partial \beta_j} \frac{\partial f}{\partial \beta_k} cov(\beta_j \beta_k) \tag{8}$$

5.1 Absolute Permeability

Klinkenberg [6] proposed a correlation between the measured permeability (apparent permeability) and absolute permeability, given by:

$$k_{ABS} = k_{AP} \left[1 + \left(\frac{b}{\bar{P}} \right) \right]^{-1} \tag{9}$$

If k_{ABS} and b are estimated by the fit of the analysis repetition at various average pressures (method 1 of section 3.1.1) the uncertainty can be estimated by the fit uncertainty (eq. 8) if the amount of measurements is large enough to be statistically representative.

If b is estimated by its correlation with the absolute permeability and k_{ABS} is calculated by the Equation (9), the propagation of uncertainty as a function of the independent sensitivity of each parameter is calculated by Equation (7).

The uncertainty of the average pressure, $\bar{P}$, must take into account the modeling of inlet and outlet pressure losses (P_D). If these losses are measured together, and the ratio between inlet pressure loss (P_{D1}) and outlet pressure loss (P_{D2}) is modeled by $R = P_{D1}/P_{D2}$, and the measured pressures are the inlet pressure (P_1) and differential pressure (ΔP), (instead of measuring outlet pressure, P_2) then:

$$\bar{P} = \frac{2\,(P_1 - R\,P_D) - (\Delta P - P_D)}{2} \tag{10}$$

The uncertainties of pressure transducers and differential pressure should come from their calibration, as discussed in Section 2.1. The uncertainty of pressure loss must originate from the modeling of pressure loss as a function of flow rate and pressure, and preferably temperature. If modeling temperature sensitivity is not feasible, tests should be conducted at the same temperature as the pressure loss correlation. Even so, a component of underestimated uncertainty will remain.

The ratio between inlet and outlet pressure losses must be modeled in some way. An analysis of the lengths of involved lines can be used in modeling, considering uncertainties in line lengths as one of the sources of uncertainty for R.

Apparent permeability is calculated based on Darcy's law, considering the measurement of P_1 and ΔP and the pressure losses in the lines, it can be written as:

$$k_{AP} = \frac{8\,P_B\,Q_B\,\mu\,L}{\pi\,D^2\,(\Delta P - P_D)\,(2\,P_1 - \Delta P + (1 - 2\,R)\,P_D)} \tag{11}$$

Where L and D are sample length and diameter, respectively, Q_B is the flow rate measured at a pressure P_B, and μ is the fluid viscosity.

The uncertainty of apparent permeability can be obtained through uncertainty propagation, as shown in Equation (7).

Another source of uncertainty for absolute permeability is the Klinkenberg parameter. Except for transient measurements, the other acquisition modes, presented in Section 3.1.1, rely on fitting correlations, which can have their uncertainties estimated from Equation (8).

When estimating the Klinkenberg parameter from a function of absolute permeability, an additional transformation is needed (to change known variable to apparent permeability) and introduce uncertainty. If the function is a power function:

$$b = C_1 k_{ABS}{}^{C_2} \tag{12}$$

From the relationship between apparent and absolute permeabilities, it is possible, through algebraic manipulation, disregarding some higher order terms, to derive the following expression for the Klinkenberg parameter as a function of known information, the apparent permeability:

$$b = \frac{\bar{P}}{2C_2} \left(-1 - \sqrt{1 + 4 \frac{C_2}{\bar{P}} C_1\, k_{AP}{}^{C_2}} \right) + O\left(C_1 \frac{b}{\bar{P}} \right) \tag{13}$$

This transformation relies on a simplification that introduces a truncation on the order of $C_1 \frac{b}{\bar{P}}$ and the resulting uncertainty is:

$$\sigma_b = \sqrt{\sum_i \left(\frac{\partial b(k_{AP}, C_1, C_2, \bar{P})}{\partial x_i} \sigma_{x_i} \right)^2} + O\left(C_1 \frac{b}{\bar{P}} \right) \tag{14}$$

5.2 Effective Porosity

Effective porosity (φ_{ef}) is typically calculated based on the relationship between the solid volume and the pore volume of the sample. These volumes are determined either through two consecutive measurements: one with the sample and one without it using the same system, or a

single measurement with the sample, combined with a calibration representing the system in the absence of the sample. All measurements and calibrations are performed using the gas expansion model described in Equation (1).

For the solid volume (V_S), the measured void volume (V_v) with the sample is referred to as the "Full Chamber Volume" or V_{FC}, while the measured void volume (V_v) without the sample, "Empty Chamber Volume" or V_{EC}. The total volume of any material added to the sample is represented by $\sum_i V_{mi}$, determined beforehand. The solid volume is then calculated as:

$$V_S = V_{EC} - V_{FC} - \sum_i V_{mi} \tag{15}$$

For the pore volume (V_P), the measured void volume (V_v) with the sample in the holder is V_{SL}. The line volume (V_L) and its uncertainty, as well as the volume of any added material (V_{vi}) must be measured beforehand, to the sample. The pore volume is given by:

$$V_P = V_{SL} - V_L - \sum_i V_{vi} \tag{16}$$

Each measurement and calibration must have its uncertainty estimated by applying the gas expansion model (Equation 1) within the uncertainty propagation equation (Equation 7).

Uncertainty in measurements can be determined based on the average of several measurements to increase the precision of the results. However, it is essential to consider the uncertainties and errors associated with two main factors: (i) temperature variations between the calibration and measurement times, as changes in temperature can affect the system's behavior and the obtained results, and (ii) operational issues, such as system assembly and equipment setup, which can introduce errors if not properly controlled. The temperature variations can be minimized using similar temperatures between calibration and measurement times or modelling the system's behavior with the temperature changes. In the later, the model and temperature uncertainties can be propagated to the final results by using the sensitivity approach (eq. 7). The operational issues have to be minimized by a proper personnel training and the uncertainty/errors introduced can't be estimated in a Type B uncertainty evaluation.

5.3 Relative Permeability

Relative permeability is defined in terms of reference permeability,

$$k_r = \frac{k_{ef}}{k_{REF}} \tag{17}$$

The uncertainty can be calculated using uncertainty propagation modeling (Equation 7).

As mentioned in Section 4.2.2, if the reference is an effective permeability point, the relative permeability at this saturation is defined as unity, with no additional uncertainty from making it dimensionless.

The uncertainty of effective permeability is calculated, in the steady-state regime, through the uncertainty propagation of Darcy's law for linear and incompressible flow.

$$k_{ef} = \frac{Q\,\mu\,L}{\pi\,D^2\left(\Delta P \pm\ \Delta\rho \cdot g \cdot L\ \cdot sin(\alpha)\right)} \tag{18}$$

Where Q is the volumetric flow rate, μ is the viscosity of the evaluated fluid, L and D are the length and diameter of the sample, respectively, ΔP is the pressure differential, $\Delta\rho$ is the fluid density difference, required if the experiment is not conducted horizontally, and α is the angle between the sample's longitudinal axis and the horizontal.

In addition to the uncertainty that can be estimated through the application of the propagation equation (7) to all observed sources in the equation, there are uncertainties associated with factors not modeled by Darcy's law, such as sample heterogeneity, instability of the advancing front, capillary edge effects, and gravitational divergence effects, as mentioned in previous sections. These sources will not be addressed in the analytical application of uncertainty propagation, but some may be considered in the numerical evaluation of confidence intervals.

In the case of relative permeability, each point carries uncertainties not only in the permeability itself but also in the representative saturation. Saturation uncertainties can be estimated based on a progression of saturation calculations or the saturation achieved as a function of cumulative production. That is, starting from an initially known saturation, (S_{fi}), the fluid saturation, (S_f), is calculated by increments or decrements in the fluid volume, ($\Delta_j V_f$), relative to the porous volume of the analyzed sample, (V_P). Thus:

$$S_f = S_{fi} + \sum_{j=1}^{N}\left(\pm\frac{\Delta_j V_f}{V_P}\right) \tag{19}$$

Applying uncertainty propagation,

$$\sigma_{S_f} = \sqrt{{\sigma_{S_{fi}}}^2 + \left(-\frac{\sum \Delta_j V_f}{V_P^2}\sigma_{VP}\right)^2 + \sum_{j=1}^{N}\left(\frac{\sigma_{\Delta_j V_f}}{V_P}\right)^2} \tag{20}$$

Another option for volume measurement in tests involving liquids without gas in solution is through the masses of the produced fluids. This type of measurement has a typical uncertainty, which depends on the difference between the densities of the produced fluids.

The volume of a one fluid V_{F1} can be calculated by

$$V_{F1} = \frac{m_T - (Q \cdot t)\rho_{F2}}{\rho_{F1} - \rho_{F2}} \tag{21}$$

From the known flow rate (Q) and time (t), produced mass (m_T) and fluids densities (ρ_{F1}, ρ_{F2}).

Care must be taken with the pressure and temperature conditions in which the flow rate and the fluid densities are provided. The uncertainties in reference pressure and temperature must also be included in the propagation analysis. Since the fluid densities are functions of temperature and pressure, and these have uncertainties in theirs measurements, the uncertainty can be propagated to

volume applying the sensitivity equation (eq. 7) to the density equations and then to the volume equation (eq. 21)

There is also the possibility of determining saturation using tomographic imaging acquisition. This type of acquisition has uncertainties related to image resolution, signal-to-noise ratio, and also characteristics of the tomography process, such as the fact that the X-ray beam in the laboratory is always polychromatic, and the choice of dopant can therefore alter the attenuation values of the rock throughout the 3D volume, and consequently, the measured saturations. In the authors' experience, saturation uncertainty through tomographic imaging is higher than that observed with volume balance methods. It is advisable, whenever possible, to perform simultaneous saturation measurements using both tomography and volumetric techniques in order to reduce the uncertainty of both measurements simultaneously.

In heterogeneous samples, the saturation profiles or 3d maps can help to improve the relative permeabilities of a porous media, but this process is quite challenging and there are ongoing R&D to propose methods to evaluate the KR for heterogeneous Brazilian rocks.

For homogeneous samples, saturation profiles may be used to evaluate the boundary effects, reducing the uncertainty of the interpretation of this phenomenon when compared with modeling the effect using a known capillary curve or optimizing one with the experimental data when possible.

5.4 Centrifuge Capillary Pressure

The capillary pressure uncertainties can be calculated applying the uncertainty propagation equation (7) in the equations 3 and 4 mentioned in Section 4.3.1

In the case of capillary pressure by centrifugation, each point of capillary pressure is related to a representative saturation, just like for relative permeability. The uncertainty of saturation in this case can be estimated in the same way described in section 5.3, taking into account the sources of measurement uncertainties cited in section 4.3.

6 Uncertainty Propagation (Numerical Approach)

6.1 Direct Modelling and Numerical Fitting

When properties are obtained through numerical model fitting to experimental data, such as relative permeability curves under transient conditions, uncertainty propagation cannot be adequately addressed using purely analytical methods. In such cases, numerical approaches based on inverse modeling and two-phase flow simulation are employed, allowing for more robust estimation of parameters and their associated confidence intervals [11,12].

The procedure involves the numerical solution of the extended two-phase Darcy equations, accounting for capillary pressure effects, fluid compressibility, and the functional dependence of properties on saturation. The model is calibrated against experimental data —such as pressure readings, produced volumes, and, when available, spatial saturation profiles— using optimization algorithms like the Levenberg-Marquardt method or sampling-based probabilistic approaches such as Markov Chain Monte Carlo (MCMC) [12,13]. The fitting process consists of minimizing an objective function, commonly defined as:

$$\chi^2 = \sum_i \left(\frac{d_i^{exp} - d_i^{model}}{\sigma_i} \right)^2 \qquad (22)$$

where d_i^{exp} represents the experimental observation, d_i^{model} is the corresponding model prediction, and σ_i is the measurement uncertainty associated with point i.

6.2 Inverse Problem Formulation

The success of this process depends directly on how the inverse problem is formulated. While the forward modeling provides the physical basis for simulating multiphase flow, it is during the inversion step that internal properties of the porous medium are inferred from observations. This formulation involves adopting reduced parametric representations for the relative permeability and capillary pressure curves, limiting the number of parameters to be estimated. Two of the most used parameterizations in this context are the Corey Model and LET Model [15].

The choice between these functions depends on the balance between representational flexibility and inversion robustness. Simpler models, such as Corey, reduce the risk of overfitting but may fail to capture more complex nonlinear behaviors. In contrast, more flexible parameterizations, like the LET model, expand the solution space but increase the risk of non-uniqueness [11,15].

Furthermore, the inverse problem is inherently ill-posed: multiple combinations of parameters may adequately reproduce the same experimental data, especially when the quantity or diversity of data is limited. This leads to solution non-uniqueness and requires that the model be properly constrained by informative data that are consistent with the physics of the system [16]. An additional challenge arises from the simplifications commonly adopted in forward modeling. Simulations are often performed in one-dimensional, homogeneous, and isotropic domains, which, although computationally efficient, may introduce bias if they do not adequately represent the actual experimental conditions. Therefore, effective inverse problem formulation requires a careful balance between model complexity, the type and amount of observational data, and the acceptable level of uncertainty in the interpretation [14].

6.3 Optimization Strategies and Uncertainty Quantification

The choice of optimization algorithm becomes a key factor in determining the quality of the solution obtained and, more importantly, in quantifying the uncertainties

associated with the estimated parameters. Different methods exhibit varying capabilities in exploring the solution space and capturing the effects of nonlinearity and parameter correlations. The Levenberg-Marquardt method, which is deterministic and gradient-based, is computationally efficient and enables uncertainty estimation through the covariance matrix, given by:

$$cov(\theta) = \sigma^2 . (J^T J)^{-1} \quad (23)$$

where J is the Jacobian matrix of the objective function with respect to the model parameters. This matrix quantifies both the individual uncertainties and the correlations between parameters, providing a clear view of the sensitivity structure of the problem. However, as a local method, Levenberg-Marquardt may converge to local minima and may not fully capture the uncertainty extent in systems with multiple plausible solutions.

To overcome these limitations, the MCMC approach has been widely adopted as a complementary tool. By sampling from the posterior probability distribution of the parameters, MCMC provides more realistic and robust credibility intervals, even in underdetermined problems or highly nonlinear settings. Studies by Berg et al. [13] show that this approach enables the identification of plausible solution regions, reveals multiple minima, and helps understand the correlation structure between estimated parameters through error ellipses and marginal distributions. The combination of both techniques, Levenberg-Marquardt for efficient fitting and MCMC for in-depth uncertainty assessment, offers a solid framework for the numerical interpretation of core flooding experiments.

Numerical uncertainty propagation is particularly valuable in scenarios where experimental data are limited or when the objective is to identify which parameter combinations are consistent with the available observations. Beyond enabling more robust interpretation, this approach can also be used predictively to guide experimental design, helping define boundary conditions and data acquisition strategies—such as multi-rate tests or in situ saturation monitoring—to enhance parameter identifiability. Recent studies by Berg et al. [11,12,13] show that, even under idealized conditions using synthetic simulations, achieving reliable solutions requires properly conditioning the inverse problem with multiple sources of information.

Results

The methodology proposed was applied to some Routine Core Analysis and, for the cases tested, the most important source of uncertainty was the sample geometry (measured by caliper, 3 times), followed by the fluid viscosity, as shown in Figure 4.

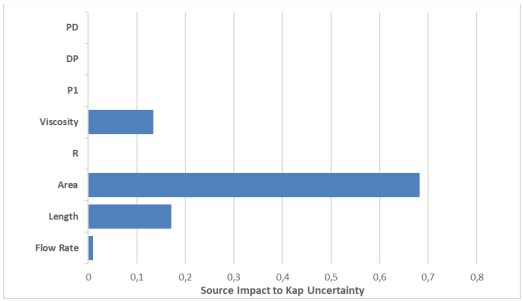

Fig. 4. Apparent Permeability Uncertainty Sensitivity.

The uncertainties of Relative Permeability sources are being used as input to the MCMC method, but the application of the sensitivity analysis can help us to understand how the different sources of uncertainty contribute to the final uncertainty.

In an USS KR analysis of a 1,5" sample (with 0,1cm caliper uncertainty), 1cm³/min flow rate (and flow rate uncertainty of 0,01cm³/min), viscosity of 6cP (with 0,15cP uncertainty) and a pressure transducer with 0,1psi uncertainty, permeabilities up to 100mD can be measured with good precision for smaller samples, but the transducer uncertainty becomes rapidly important for higher permeabilities, what can be seen at Figure 5.

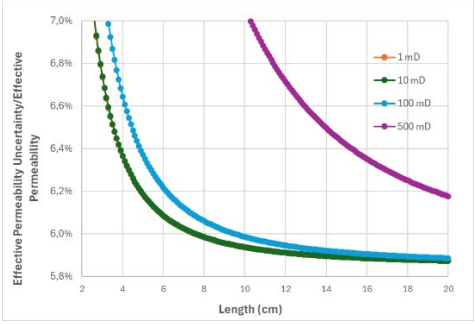

Fig. 5. Effective Permeability Uncertainty Sensitivity to the Sample Length.

For the same data mentioned above, but fixing sample length in 5cm, analyzing the sensitivity to the flow rate, it can be seen (fig. 6) that for flow rates above 0,5cm³/min and absolute permeabilities bellow 100mD, the uncertainties are reasonably low. Bellow 10mD there is no improvement on uncertainty due to sources that does not depend on differential pressure.

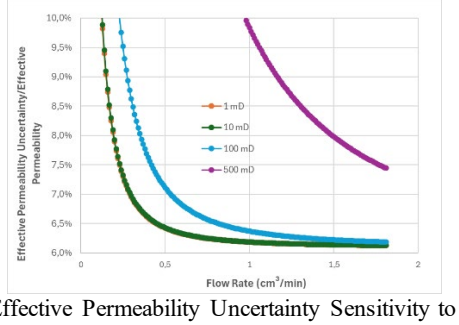

Fig. 6. Effective Permeability Uncertainty Sensitivity to the Flow Rate.

In a KR USS test of sample with Pore Volume uncertainty of 0,1cm³, and the equipment with volume measurement uncertainty of 0,1cm³, an inlet dead volume of 0,5 cm³ and an outlet dead volume of 1,0cm³ (both with 0,1cm³ uncertainty) the (total not relative) saturation uncertainty increases through test time as shown in Figure 7. At the

test beginning and after each change in saturation direction, the dead volumes increase significantly the total uncertainty.

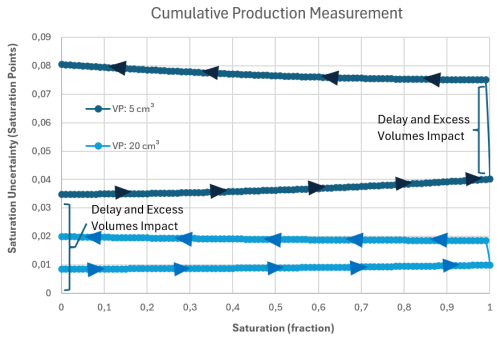

Fig. 7. Saturation uncertainty increase through time.

If the volume was measured step by step, the scenario would be worse, since each measurement uncertainty would be added to the final uncertainty.

Conclusion

There are numerous sources of uncertainty in routine and special core analysis tests, and these uncertainties interact with the properties measured in complex ways, making the estimation of uncertainties a highly intricate task.

Within the scope of this article, some of those uncertainties were analyzed, and methods for quantifying the resulting uncertainties were reviewed or proposed. However, further exploration of these sources and the processes of uncertainty propagation would require considerably more space and examples. Nonetheless, based on the insights provided in this study, it is possible to establish a framework for estimating uncertainties in basic and special petrophysical analyses.

A careful assessment of uncertainty sources and their impact on the resulting uncertainties enables laboratories involved in rock property characterization to focus on reducing the most critical uncertainties while avoiding analyses where the levels of uncertainty result in non-representative values. Moreover, this evaluation is crucial for data users, who can incorporate measured property uncertainties into reservoir models, thereby yielding more reliable confidence intervals in reserve estimation and production scenario forecasting.

Acknowledgments

This work would not have been possible without the participation of the special and routine core analysis groups at CENPES/Petrobras, especially researchers Cindi de Oliveira Gehlen and Ana Paula Palhares Simoncelli.

References

1. McVay, D.A.; Dossary, M.N. The Value of Assessing Uncertainty (SPE 160189); SPE Annual Technical Conference and Exhibition; San Antonio, Texas, USA (2012)
2. Yaslam, M.; Ghedan, S.G.; Kalam, Z. Revealing Relative Permeability Uncertainties through Integrated Experimental and Modeling Workflow; SPE Reservoir Characterisation and Simulation Conference and Exhibition, Abu Dhabi, UAE (2013)
3. JCGM 100:2008 (corrected GUM 1995) – Evaluation of measurement data – Guide to the expression of uncertainty in measurement;
4. Rücker, Maja et al. The Origin of Non-thermal Fluctuations in Multiphase Flow in Porous Media (671399); Frontiers in Water (2021)
5. De Groot, M., & Schervish, M. Probability and Statistics. Boston: Pearson Education Inc. (2012)
6. Klinkenberg, L.J. The Permeability of Porous Media to Liquids and Gases. Drill. & Prod. Prac.200 (1941)
7. Jones Stanley C. A Rapid Accurate Unsteady-State Klinkenberg Permeameter (SPE-3535) // SPE 46th Annual Fall Meeting. New Orleans (1972).
8. Subbey Sam, Christie Mike and Sambridge Malcolm The Impact of Uncertain Centrifuge Capillary Pressure on Reservoir Simulation // SIAM Journal on Scientific Computing. - Philadelphia Vol. 26 (2004)
9. Forbes Pierre L. Simple and Accurate Methods for Converting Centrifuge Data Into Drainage and Imbibition Capillary Pressure Curves // The Log Analyst - pp. 31-53. - 0024-581X (1994).
10. Michelon Mateus Fontana [et al.] Incerteza de Medição de Propriedades Petrofísicas de Quatro Amostras Medidas em Porosímetro e Permeâmetro (RT OEXP-M-AGUP/LAB 001/19)- Santos: Petrobras Internal Report [Restricted access], (2019).
11. Berg, S. et al. Sensitivity and uncertainty analysis for parameterization of multiphase flow models. Transport in Porous Media, v. 140, p. 27–57, (2021).
12. Berg, S., et al. "Uncertainty quantification of relative permeability from core flooding via inverse modeling." Transport in Porous Media, 135, 449–469, (2020).
13. Berg, S. et al. Simultaneous determination of relative permeability and capillary pressure from an unsteady-state core flooding experiment? Computers and Geotechnics, v. 168, p. 106091, (2024).
14. Carrassi, A. et al. Data assimilation in the geosciences: An overview of methods, issues, and perspectives. Wiley Interdisciplinary Re-views: Climate Change, v. 9, n. 5, p. e535, (2018).
15. Lomeland, F.; Ebeltoft, E.; Thomas, L. K. A new versatile relative permeability correlation. In: SPE Annual Technical Conference and Exhibition. Proceedings. Dallas: Society of Petroleum Engineers. SPE 99326, (2005).
16. Oliver, D. S.; Reynolds, A. C.; Liu, N. Inverse theory for petroleum reservoir characterization and history matching. Cambridge: Cambridge University Press, (2008).